Colloidal Particle Scattering: A New Method To Measure Surface Forces

T. G. M. van de Ven,* P. Warszynski,† X. Wu, and T. Dabros‡

Paprican and Department of Chemistry, Pulp and Paper Research Centre, McGill University, Montréal, Canada H3A 2A7

Received June 15, 1994[⊗]

A new method for determining the forces between colloidal particles is presented, based on observing the changes in two-particle collision trajectories in a linear shear flow and inverting the trajectory equations describing such collisions. In the absence of colloidal forces and under low Reynolds number conditions, collisions are symmetric and reversible. When colloidal forces are acting between the particles, this symmetry is broken, and the degree of asymmetry is a measure of the magnitude of colloidal forces. From a sufficiently large number of experimentally observed collision trajectories we can determine the colloidal forces by a minimization method, assuming some relationship between the interaction force and interparticle distance. This relationship can either be taken from theory, e.g., classical DLVO theory, or be represented by a general function of interparticle distance with adjustable parameters which can be determined from the best fit between theory and experiment. From Monte Carlo simulations it has been found that the number of collisions required for a reliable determination of the colloidal force–distance relationship is about 25. Some experiments have been done with a "surface collision apparatus", which we describe in detail. The results for latex particles in mixtures of glycerol–water and D_2O–water show that the method is capable of detecting forces that are 3–4 orders of magnitude smaller than those measured by a conventional surface force apparatus or by atomic force microscopy. A minimization analysis of data obtained previously with the traveling microtube apparatus is also presented.

Introduction

Determination of interaction forces between particles is a fundamental problem in colloid science, as the way the force varies with interparticle distance determines various properties of a colloidal system. By adding electrolytes, neutral polymers, or polyelectrolytes to a suspension or letting them adsorb on particle surfaces, one can change the interaction forces between particles and thus change the stability or the rheological behavior of the system.

The most direct method of determining interaction forces was developed by Israelachvili and Tabor.[1] The method is based on the measurement of the interaction forces between crossed macroscopic mica cylinders which can be accurately positioned within a separation distance from a fraction of a nanometer to 1 μm. The distance is obtained from the interference pattern of laser light, and the force is calculated from the compression of the spring to which one of the cylinders is attached. The experimental apparatus, usually called "surface force apparatus" (SFA), is now commercially available, and many results for interaction forces in various systems have been published.[2] However, there are some drawbacks of this method: (i) Although the distances between interacting surfaces are in the range typically encountered in colloidal systems, measurement is possible only for macroscopic mica surfaces and not for real colloidal particles; (ii) SFA is not sensitive enough to measure the force close to the secondary energy minimum, which is often the most crucial part for a colloidal system; (iii) usually only the static forces, i.e., forces with a characteristic time longer than a second, can be measured, whereas the characteristic time for a Brownian collision of 1 μm particles is of the order of 10^{-4}–10^{-3} s. The dynamic forces acting between particles during a collision can be very different from static ones. The hysteresis observed in some experiments[3] measuring interaction forces between two polymer surfaces may be attributed to the influence of the relaxation of polymer conformation on the measured force. Recent technical improvement allows a vibrational motion of one of the surfaces and thus enables SFA to measure dynamic forces.[4] However, the piezoelectric bimorph does not improve the sensitivity of measurement, and the vibrational frequency is limited by the natural frequency of the bimorph, which is on the order of 100 Hz.

Another widely used method of force measurement is atomic force microscopy (AFM).[5] It measures forces either between a standard AFM tip of the microscope probe (usually a Si_3N_4 crystal) and a macroscopic surface[6,7] or between a colloidal particle glued to the end of the cantilever and the surface.[8,9] Recently, an attempt has been made to measure forces between two latex particles.[10] Depending on the operating mode of the AFM, one can measure either static or dynamic forces with a characteristic time longer than 0.1 s, since the probe can scan a distance of 100 nm with a frequency of several hertz. The sensitivity of the AFM method is limited by the spring constant of its cantilever and the accuracy of the cantilever deflection measurement. For a typical spring constant of the order of 0.1 N/m, and a deflection of 0.1 nm, one can measure a force of the order of 10^{-11} N. Like SFA, this force is 3–4 orders of magnitude larger than the interac-

† Current address: Institute of Catalysis and Surface Chemistry, Polish Academy of Sciences, 30-239 Krakow, Poland.

‡ On leave from Jagiellonian University, Krakow, Poland. Current address: CANMET, One Oil Patch Drive, P.O. Bag 1280, Devon, Alberta, Canada T0C 1E0.

[⊗] Abstract published in *Advance ACS Abstracts,* August 15, 1994.

(1) Israelachvili, J. N.; Adams, G. E. *J. Chem. Soc., Faraday Trans. 1* **1978**, *74*, 975.

(2) Israelachvili, J. N. *Intermolecular and Surface Forces*, 2nd ed.; Academic Press: San Diego, 1992.

(3) Marra, J.; Hair, M. L. *J. Colloid Interface Sci.* **1988**, *125*, 552.

(4) Israelachvili, J. N.; Kott, S. J. *J. Polym. Sci., Part B: Polym. Phys.* **1989**, *27*, 489.

(5) Binnig, G.; Quate, C. F.; Gerber, Ch. *Phys. Rev. Lett.* **1986**, *56*, 930.

(6) Hartmann, U. *Phys. Rev. B* **1991**, *43*, 2404.

(7) Weisenhorn, A. L.; Hansma, P. K.; Albrecht, T. R.; Quate, C. F. *Appl. Phys. Lett.* **1989**, *54*, 2651.

(8) Ducker, W. A.; Senden, T. J.; Pashley, R. M. *Nature* **1991**, *353*, 239.

(9) Butt, H.-J. *Biophys. J.* **1991**, *60*, 1438.

(10) Li, Y. Q.; Tao, N. J.; Garcia, A. A.; Lindsay, S. M. *Langmuir* **1993**, *9*, 637.

0743-7463/94/2410-3046$04.50/0 © 1994 American Chemical Society

tion force around a secondary energy minimum. Moreover, the capability of the dynamic force measurement is limited by the low vibrational frequency of the tip.

Other direct force measurement methods are the micropipet method,[11] the osmotic stress method,[12] and the osmotic pressure method.[13] All of them measure static equilibrium forces. The micropipet method does not give any interaction force–distance relationships. It only measures the surface affinity at one separation distance. Furthermore, it is limited to membrane systems. The osmotic stress method is limited to the study of multilayer materials. Neither of them can be applied to study any commonly used polymers or colloids. The osmotic pressure method actually measures the interaction forces between latex particles, but the force profile depends on the assumed crystal model, which is not exactly the same as that in a real concentrated latex suspension containing both ordered and disordered structures. Therefore, the interpretation of the results is open to discussion.

It is also possible to obtain the interaction forces indirectly by correlating experimentally obtained coagulation rates with theoretical predictions. In that case, however, reliable results can only be obtained for monodisperse particles, provided that the initial concentration of particles is known. The same restrictions apply to the method of determining the interaction forces from deposition experiments.[14] The latter method has the advantage that deposition rates can be visually measured, so the results are more reliable than those from coagulation experiments. Deposition rates can later be correlated to theoretical predictions to give the interaction forces. Limitations of the method are discussed in ref 15.

Some other methods involve finding the interaction energy profile for a particle near an interface and then calculating the force by differentiation. This can be achieved by using evanescent wave spectroscopy techniques to find the concentration profile of colloidal particles at an interface, which, in the case of dilute suspensions, is related to the interaction energy by the Boltzmann distribution.[16] Another method involves studying the Brownian motion of particles near an interface.[17–19] From the amplitude of Brownian displacements in the neighborhood of the secondary minimum, one can find the shape of the interaction energy profile. These two methods indeed measure forces in the most important region of a force–distance profile, but they are limited to measuring the static interactions beween a particle and a surface only.

The energy–distance relationship can also, in principle, be calculated from the pair correlation function, which can be calculated from the structure factor obtained from static light scattering experiments.[20] Because of the complication of the model and calculation procedures, only limited success has been achieved.[21]

In this paper we present a new method of force measurement which we call colloidal particle scattering (CPS). The method is analogous to elementary particle (e.g. electrons) scattering, which can be used to evaluate the interactions between elementary particles by studying the distribution of impact parameters and deflection angles of collisions. However, elementary particle scattering cannot really quantitatively determine the particle–particle interactions because the exact trajectory of each collision is unknown. CPS does not have such a problem. Every individual collision trajectory is accurately measured. In different collisions, e.g. a head-on collision or a grazing collision, particles "sample" different regions of the interaction force profile, and obtaining a sufficient number of different collisions allows one to determine the full force profile. The procedure of obtaining the force profile from collisions with the CPS method is called trajectory inversion. The inversion is done by assuming some functional force–distance relationship with several adjustable parameters and fitting them by matching the calculated trajectories and the experimental trajectories using a least squares method. Brownian motion of particles and experimental errors may cause deviations in particle trajectories. To obtain a reliable fit, the number of collision trajectories should well exceed the number of parameters to be fitted. A Monte Carlo simulation of the experiment has been done to determine the minimum number of collisions required to invert the trajectory equation at a given level of experimental error.

The CPS method has the advantage that interaction forces are measured between real colloidal particles instead of macroscopic surfaces. Dynamic forces can be easily determined since the meaurement is done with moving particles. The relative approach velocity of a particle is around 10 μm/s, equivalent to the maximum velocity that can be achieved by a SFA operating in a dynamic mode. The approach velocity of CPS can be even higher if a high-speed video system is used. Moreover, the CPS method is far more sensitive than SFA and AFM methods. It can detect forces which correspond to interaction energies of a single kT. With this capability, it can determine the force–distance relationship around a secondary energy minimum accurately.

To illustrate the usefulness of our trajectory inversion technique used in CPS, we include some reanalysis of the collision data obtained previously with the traveling microtube apparatus.[22,23] That apparatus is based on the same idea as CPS, but with it one cannot easily observe enough collisions in a single experiment to invert the trajectory equation reliably.

In this paper we present a new experimental setup which we call a "surface collision apparatus", to replace the traveling microtube. It is based on microscopic observations of the relative motion of two colloidal particles. One particle is attached to a surface, and the other one moves along the surface in a wall shear flow to collide with the stationary one. With this apparatus it is possible to create a sufficiently large number of collisions between two particles. The collision trajectories are analyzed by image analysis. The interaction force between the particles is calculated with the trajectory inversion technique mentioned above. Some preliminary results show that the force–distance profile can be accurately determined by this method.

(11) Evans, E. A. *Biophys. J.* **1980**, *31*, 425.
(12) Parsegian, V. A.; Rand, R. P.; Fuller, N. L. *J. Phys. Chem.* **1991**, *95*, 4777.
(13) Rohrsetzer, S.; Kovács, P.; Nagy, M. *Colloid Polym. Sci.* **1986**, *264*, 812.
(14) Dabros, T.; van de Ven, T. G. M. *Colloid Polym. Sci.* **1983**, *261*, 694.
(15) Adamczyk, Z.; Dabros, T.; Czarnecki, J.; van de Ven, T. G. M. *Adv. Colloid Interface Sci.* **1983**, *19*, 183.
(16) Schumacher, G. A.; van de Ven, T. G. M. *Langmuir* **1991**, *7*, 2028.
(17) Alexander, B. A.; Prieve, D. C. *Langmuir* **1987**, *3*, 778.
(18) Prieve, D. C.; Frej, N. A. *Langmuir* **1990**, *6*, 396.
(19) Rädler, J.; Sackmann, E. *Langmuir* **1992**, *8*, 848.
(20) Hunter, R. J. *Foundations of Colloid Science*; Clarendon Press: Oxford, 1989; Vol. 2.
(21) Hirtzel, C. S.; Rajagopalan, R. *Colloidal Phenomena—Advanced Topics*; Noyes Publications: Park Ridge, NJ.
(22) Takamura, K.; Goldsmith, H. L.; Mason, S. G. *J. Colloid Interface Sci.* **1981**, *82*, 175.
(23) Takamura, K.; Goldsmith, H. L.; Mason, S. G. *J. Colloid Interface Sci.* **1981**, *82*, 190.

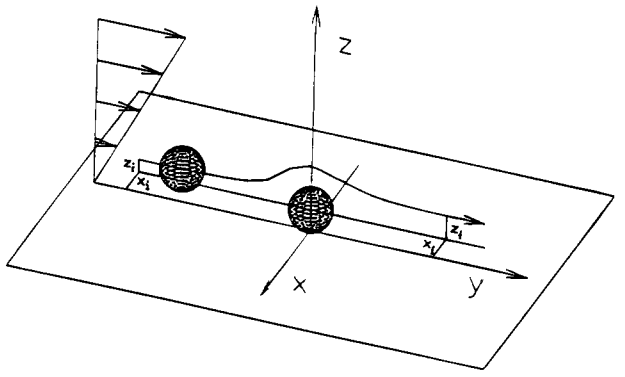

Figure 1. Illustration of a colloidal particle collision. The particle in the center is stuck to the wall. A second particle is moving toward it to undego a collision. The collision trajectory, illustrated by the curve with an arrow at the end, can be represented by the initial position (x_i,z_i) of the moving particle before the collision and the final position (x_f,z_f) of the particle after the collision.

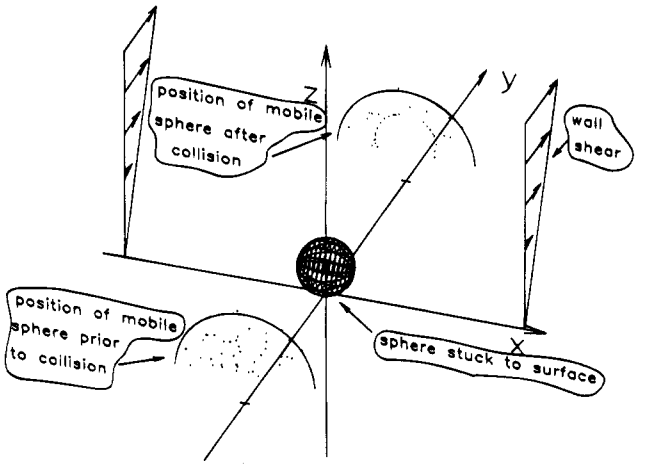

Figure 2. Illustration of the basic principles of the CPS method. The initial and final positions of a moving particle (cf. Figure 1) for many collisions are plotted in a "scattering pattern". Different interaction force vs interparticle distance profiles will lead to different scattering patterns. From an experimentally determined scattering pattern, it is possible to calculate the force–distance profile with the trajectory inversion technique.

Basic Principles

1. Inversion of Trajectory Equation. The principle of the method is illustrated in Figures 1 and 2. One latex particle is stuck to a surface, and another one moves toward it in a wall shear flow. The origin of the coordinate system is placed on the surface right below the center of the stationary particle. If the Brownian motion of the particles is neglected, the trajectory equation of the moving particle is, in general, given by

$$\frac{d\mathbf{r}}{dt} = \mathbf{M}\cdot(\mathbf{F}_{hydr} + \mathbf{F}_{int}) \qquad (1)$$

where $\mathbf{r}$ is the position vector of the moving particle, t is the time, $\mathbf{M}$ is the mobility tensor, $\mathbf{F}_{hydr}$ is the hydrodynamic force, and $\mathbf{F}_{int}$ is the interaction force between two particles, which consists of several contributions such as van der Waals forces, electric double-layer forces, steric forces, electroviscous forces, etc.

The mobility matrix and hydrodynamic force are generally a function of the particle coordinates which can be found from the solution of the Navier–Stokes equation. Since in colloidal systems the Reynolds number, based on the flow velocity, the dimensions of the particles, and the viscosity of the medium, is almost always much smaller than 1, one can neglect inertia effects and use the creeping flow equation instead.

Equation 1 describes the evolution of the relative positions of the moving particle with time. By knowing the initial position of the particle and the interaction forces, one can predict its final position after the collision. When two particles are far apart, the moving particle follows the direction of the flow, and the x and z coordinates (cf. Figure 1) of the particle remain constant. Therefore, it is sufficient to describe the collision trajectory in terms of the initial position, (x_i,z_i), and the final position, (x_f,z_f), and the collision can be formally expressed as a transformation in the complex plane $Z_i \rightarrow Z_f$, where $Z_i = x_i + iz_i$ and $Z_f = x_f + iz_f$ $(i = \sqrt{-1})$. If we assume that the interaction force is given by some function of distance between particles, $\mathbf{F}_{int} = \mathbf{F}_{int}(\mathbf{r}, A_1, ..., A_N)$, where A_i are parameters, we can calculate the theoretical final positions of the moving particle from the experimentally given initial positions and adjust the set of parameters A_i to match them to the experimental final positions.

The fitting procedure is accomplished by minimizing the χ^2 function defined as

$$\chi^2 = \sum_{i=0}^{J} \frac{(Z_f^{th} - Z_f^{exp})_i (Z_f^{th} - Z_f^{exp})_i^*}{(\Delta Z_f^{exp})_i (\Delta Z_f^{exp})_i^*} \qquad (2)$$

where J is the number of experimental trajectories, Z_f^{exp} is the experimental final position of the moving particle expressed as a complex number, Z_f^{th} is the theoretical final position calculated from the initial position Z_i by solving the trajectory equation, and ΔZ_f^{exp} is the error in the final position, which consists of the experimental error in measuring the particle position and possible displacements due to Brownian motion during the collision. The asterisk indicates the complex conjugate. A standard procedure like the Marquart–Levenberg algorithm[24] is used for the minimization.

The set of parameters A_i for which χ^2 attains a minimum describes the interaction force profile. The goodness of fit is characterized by the value of χ^2 for J-N-1 degrees of freedom, where N is the number of parameters. The confidence intervals for the parameters can be calculated in the usual way using a covariance matrix.

For traveling microtube experiments,[22,23] the basic principle is the same except that the wall shear flow is replaced by a simple shear flow and the stationary particle is replaced by a freely rotating particle.

2. Error Analysis. Since the position of a particle is measured with some experimental errors, it is necessary to analyze how the errors affect the resulting interaction force profile. This was done by a Monte Carlo simulation method. To speed up the calculation, only collisions in a simple shear flow (observed with the traveling microtube) were simulated. In such a system the trajectory equation of the moving particle (cf. eq 1) can be simplified considerably. For equal-sized spheres the trajectory equation can be expressed in spherical coordinates as[25]

$$\frac{dr}{dt} = GA(r)\sin^2\theta \sin 2\phi + \frac{kTC(r)\bar{F}_{int}(r)}{3\pi\mu a^2}$$

$$\frac{d\theta}{dt} = \frac{1}{4}GB(r)\sin 2\theta \sin 2\phi$$

(24) Press, W. H.; Flannery, B. P.; Teukolsky, S. A.; Vetterling, W. T. *Numerical Recipes—The Art of Scientific Computing*; Cambridge Univ. Press: Cambridge, 1987.

(25) van de Ven, T. G. M.; Mason, S. G. *J. Colloid Interface Sci.* **1976**, *57*, 505.

$$\frac{d\phi}{dt} = \frac{1}{2}G(1 + B(r)\cos 2\phi) \quad (3)$$

where r is the dimensionless distance between particles scaled by the particle radius a, G is the shear rate, μ is the viscosity, and $A(r)$, $B(r)$, and $C(r)$ are known functions of r.[25-27]

The interaction force was assumed to be of the DLVO type.[28,29] In dimensionless units of kT/a (k is the Boltzmann constant and T is the temperature), it can be expressed as

$$\bar{F}_{int}(H) = \mathrm{Dl}\tau\exp(-\tau H) - \frac{\mathrm{Ad}}{2H^2}f(\mathrm{Al},H) \quad (4)$$

with

$$f(\mathrm{Al},H) = \begin{cases} \dfrac{1 + 3.54p}{(1 + 1.77p)^2} & \text{for } p < 1 \\ \dfrac{0.98}{p} - \dfrac{0.434}{p^2} + \dfrac{0.067}{p^3} & \text{for } p \geq 1, p = \mathrm{Al}H \end{cases} \quad (4a)$$

where $\tau = \kappa a$ (κ being the Debye parameter), Dl is the double-layer interaction parameter defined as $\mathrm{Dl} = 32\pi\gamma_0^2\epsilon akT/(ze)^2$ (ϵ being the permittivity of the medium, ze the ionic charge, $\gamma_0 = \tanh(ze\psi_0/4kT)$, ψ^0 being the surface potential of the particle), $\mathrm{Ad} = A/6kT$ (A is the Hamaker constant), and $\mathrm{Al} = 2\pi a/\lambda$ (λ is the characteristic wavelength accounting for the effect of retardation).

A DLVO interaction force profile with a deep secondary minimum (cf. solid lines in Figures 3 and 4) was chosen, because the trajectories would then be very sensitive to the changes of initial positions, so the effect of position errors is pronounced. The procedure of the analysis is as follows: first, a set of initial positions of the moving particle was randomly generated, and the trajectory equation with the assumed force profile was solved to obtain the final positions of the particle. Then the values of the initial and final positions were spread around the original ones according to a normal distribution with a variance equal to the square of the experimental error. Finally, a force curve was calculated from the new initial and final positions of the moving particle. This procedure was repeated several times, and the resulting force profiles are represented by the dashed lines in Figures 3 and 4. Ideally, to obtain a good reproducibility of the original force curve (solid lines in the figures), it is necessary to have at least 60 trajectories for a 6% error (relative to particle radius) or 30 trajectories for a 3% error. However, due to the limit of the computational power of the present computer (IBM 386 with AT-super coprocessor board from YARC system corporation), fewer collisions are actually used in the fitting. Usually we consider the scattering in the fitted force profiles in Figure 4a (with only 15 trajectories) still tolerable, so 20–25 collisions will be enough for a 6% error.

The error results from Brownian motion, misalignment, and external noise. Brownian motion is the main contribution to the error. It affects both the position measurement before and after a collision and the collision trajectory itself during a collision (resulting in an error after the collision). As will be shown later, both effects can be minimized by certain data processing procedures.

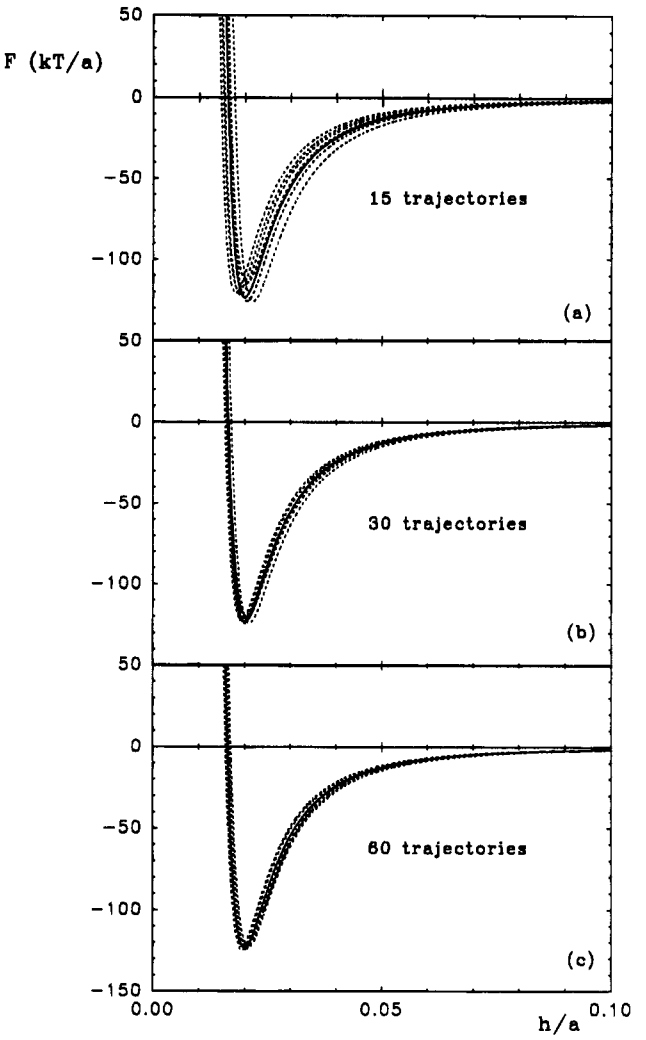

Figure 3. Effects of experimental errors, assumed to be 3%, on force–distance profiles evaluated by Monte Carlo simulations. The solid curves are the force–distance profiles used in generating the trajectories, while the dotted curves are obtained by the trajectory inversion technique. The numbers of collision trajectories used in the fitting are (a) 15, (b) 30, and (c) 60.

The latter effect, however, remains much bigger than the former one even after the processing. Its magnitude can be evaluated from

$$\Delta_{x,z}^{\mathrm{Br}} = \sqrt{\frac{2D_{x,z}a}{V_p}} \quad (5)$$

where V_p is the velocity of the moving particle and $D_{x,z}$ is the diffusion coefficient of the particle in two directions perpendicular to the flow. Equation 5 determines the minimum size of particles for which the collision experiment is still feasible. In aqueous solution this minimum size appears to be around 4 μm. On the other hand, using very big particles may decrease the sensitivity of detecting interaction forces since the ratio of colloidal to hydrodynamic forces decreases with increasing particle size. It has been found by trial and error that the optimal partizle size in an aqueous system is around 5 μm. The optimal particle size in other systems can be scaled accordingly from the relative viscosities of the systems to water, based on the Stokes–Einstein relationship between diffusion coefficient and viscosity. With the optimal particle size, the error in the final position is still larger than 10% of the particle radius due to the Brownian motion effect during a collision. After certain selection procedures (to be discussed later), this error can be reduced to about

(26) Arp, P. A.; Mason, S. G. *J. Colloid Interface Sci.* **1977**, *61*, 21.
(27) Batchelor, G. K.; Green, J. T. *J. Fluid Mech.* **1972**, *56*, 375.
(28) Vervey, E. J.; Overbeek, J. Th. G. *Theory of Stability of Lyophobic Colloids*; Elsevier: Amstredam, 1948.
(29) Schenkel, J. H.; Kitchener, J. A. *Trans. Faraday Soc.* **1960**, *56*, 161.

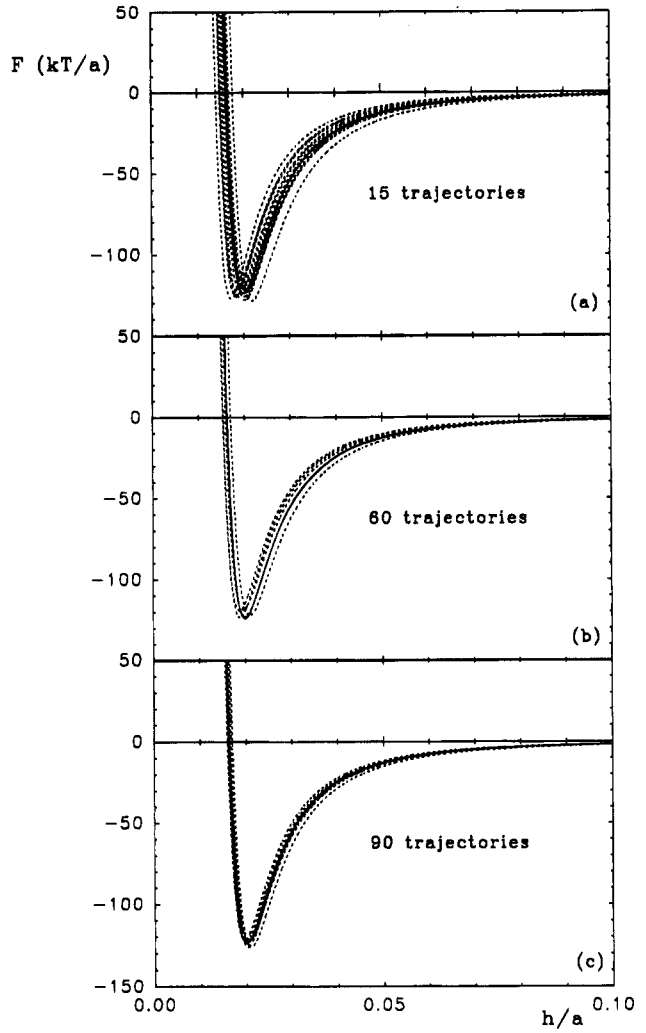

Figure 4. Effects of experimental errors, assumed to be 6%, on force–distance profiles evaluated by Monte Carlo simulations. The meanings of solid and dotted curves are the same as in Figure 3. The numbers of collision trajectories used in the fitting are (a) 15, (b) 60, and (c) 90.

10% of the particle radius. Taking into account that the error in the initial position is much smaller (about 2%; see Experimental section for details), the average error in initial and final positions is around 6%. As mentioned above, for such an error 20–25 collisions are sufficient to fit a force profile curve.

3. Choice of the Form of the Interaction Force. When the shape of the function $\mathbf{F}_{int}$ is known from theory (e.g. DLVO theory), the most convenient choice of the parameters A_i is the one corresponding to the theoretical parameters like Hamaker constant, double-layer thickness, etc. If the nature of the interaction is unknown, $\mathbf{F}_{int}$ can be chosen as a general function of interparticle distance given by a series of some orthogonal functions, e.g., a Fourier series, a Chebyshev expansion, or any other polynomial expansion, with adjustable weighting coefficients. For many colloidal systems, the form of the DLVO force is usually good enough to represent the real interaction force.

The validity of the force form given by DLVO theory has been confirmed by fitting the collision data in the simple shear flow system. The fitted force–distance profiles are shown in Figure 5. Three kinds of force–distance relationships were tried. The solid curve represents the DLVO force. The dashed curve represents the polynomial form of 12th order. The dotted curve represents a combination of an exponential term and a 10th-order polynomial term. Since the latter two forms are arbitrary, the similarity in shape between the curves given by these two force–distance relationships and the curve given by DLVO theory proves that the DLVO expression for the force is valid for systems with bare latex particles. For systems containing polymer-coated particles, a DLVO expression can still be used because its exponential repulsion term can represent either double-layer repulsion or steric repulsion or both.[30]

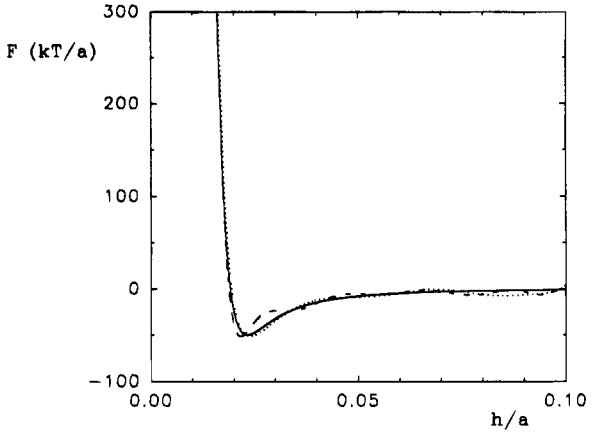

Figure 5. Comparison of various force–distance curves fitted from the same set of collision data for 2.6 μm polystyrene latex particles suspended in a 50% glycerol–water solution with a salt (KCl) concentration of 10^{-2} M, subjected to simple shear flow. The solid curve represents the DLVO force–distance expression. The dashed curve represents a polynomial form of 12th order. The dotted curve represents a combination of an exponential term and a 10th-order polynomial term.

Collisions in a Simple Shear Flow

Experimental data of particle collision trajectories given by Takamura et al.[22,23] with the traveling microtube apparatus were reanalyzed to test our trajectory inversion technique. In these experiments collisions between 2.6 μm polystyrene latex particles were observed in a 10 mM KCl solution containing 50% glycerol to suppress the Brownian motion of the particles. A cationic polyelectrolyte "Cat-floc" was then introduced into the system, and different trajectories were observed. The description of the apparatus, the experimental procedure, and the method of finding particle positions before and after a collision are given elsewhere.[22,23]

Since there were not enough experimental data available (less than 10 trajectories in each experiment), we restricted ourselves to fit only two parameters, Dl and Ad (cf. eq 4). The retardation parameter has a small influence on the shape of the force–distance curve. A value corresponding to $\lambda = 100$ nm was assumed. The value of τ was determined by the ionic strength of the suspension and was fixed in the minimization procedure. The results of the inversion of the trajectory equation for three systems are shown in Figure 6a–c. The soft-wall repulsion in the absence of polyelectrolyte reflects the electric double-layer interaction. A shift of the soft-wall repulsion for solutions containing polyelectrolyte indicates the superposition of double-layer and steric repulsion. The fitted Hamaker constant (calculated from Ad) in Figure 6a,b is 4.4×10^{-21} J, and the fitted surface potential (calculated from Dl) is −43 mV. Takamura et al.[22] quoted a Hamaker constant of 2.7×10^{-21} J from theoretical calculations and a ξ-potential of −45 mV from microelectrophoresis experiments. The fitted surface potential in Figure 6c is +39

(30) Napper, D. H. *Polymeric Stabilization of Colloidal Dispersions*; Academic Press: London, 1983.

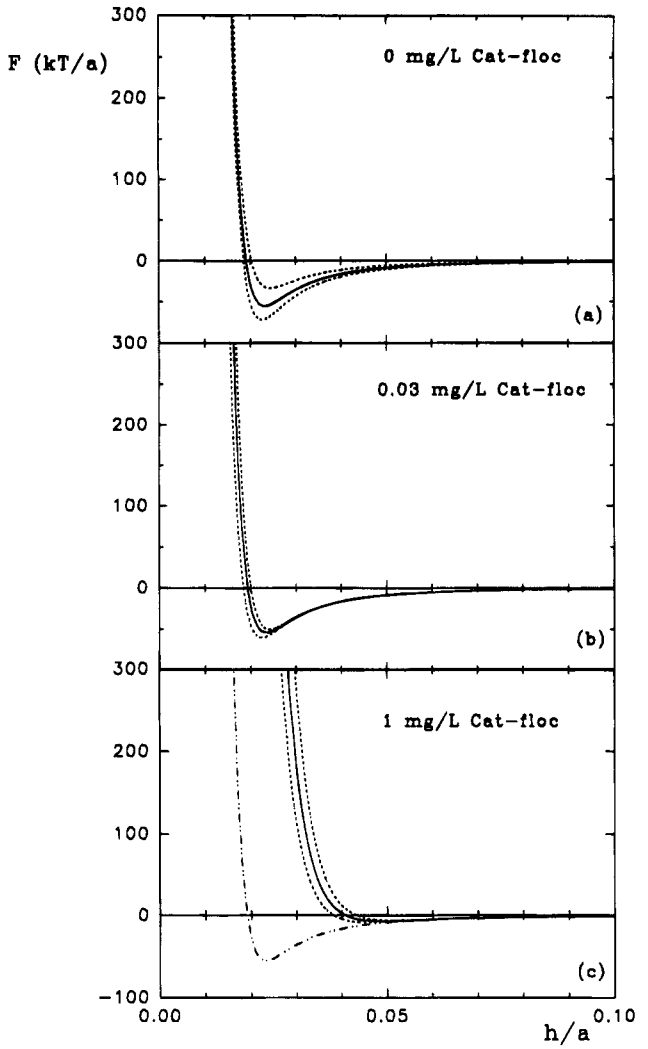

Figure 6. Fitted force–distance profiles from traveling microtube data using the trajectory inversion technique. Polystyrene latex particles (2.6 μm) were used to study the effects of a polyelectrolyte (Cat-floc) on force–distance profiles in a 50% glycerol–water solution with 10^{-2} M KCl. The dotted curves are the 90% confidence limits. (a) No Cat-floc was added. (b) 0.03 mg/L Cat-flox was added. (c) 1 mg/L Cat-floc was added. The dashed line in part c is the result of part a (in the absence of polyelectrolyte) used for comparison. The distance between this line and the solid line is an indication of the thickness of the adsorbed polyelectrolyte layer.

mV, and the ξ-potential from Takamura's measurement[23] is +35 mV. The agreement between our fitting results and the literature values shows that the trajectory inversion technique is really capable of extracting the interaction force profile from particle collisions.

Collisions in a Wall Shear Flow

The main drawback of the traveling microtube technique is its low efficiency in generating collisions. One is unable to observe a sufficient number of collisions to satisfy the conditions of statistical significance for the inversion of the trajectory equation. In this section we propose a new experimental technique using a surface collision apparatus. It increases the efficiency by at least 3 orders of magnitude, and its trajectory measurement is far more accurate than for the traveling microtube technique since both coordinates of a particle position can be measured directly instead of being fitted.[22] The surface collision apparatus creates particle collisions in a wall shear flow (cf. Figure 1). Since one particle is kept stationary, one can easily control the collisions (to make a head-on collision or a grazing collision, for example). Hence, not only is the number of collisions greatly increased compared with the traveling microtube technique, but the quality of the collisions is improved as well.

The basic principles have already been discussed above. In this section a more detailed description about the trajectory equation is given.

The components of the mobility matrix in the trajectory equation (eq 1) are found by solving the linearized, steady-state Navier–Stokes equation:

$$\mu\nabla^2\mathbf{v} = \nabla p$$

$$\nabla\cdot\mathbf{v} = 0 \tag{6}$$

where $\mathbf{v}(x)$ is the fluid velocity vector at point x and p is the pressure.

If we consider a system bounded by a stationary wall with an undisturbed fluid flow field given by $\mathbf{v}^0(\mathbf{x})$, the solution of eq 6 for two solid particles can be written as

$$\mathbf{v}(\mathbf{x}) = \mathbf{v}^0(\mathbf{x}) + \sum_{i=1}^{2}\int_{S_i}\tau(x,y)\cdot\mathbf{f}(y)\,d\mathbf{S}(y) \tag{7}$$

where $\mathbf{f}(y)$ is the force density at a point y of the particle surface. The no-slip boundary conditions at the wall can be satisified by choosing a proper expression for the Oseen tensor $\tau(x,y)$.[31,32]

The total force $\mathbf{F}_j$ and torque $\mathbf{T}_j$ exerted by the particle j (j = 1,2) on the fluid are given by

$$\mathbf{F}_j = \int_{S_j}\mathbf{f}(y)\,d\mathbf{S}(y)$$

$$\mathbf{T}_j = \int_{S_j}(y - \mathbf{r}_j)\mathbf{f}(y)\,d\mathbf{S}(y) \tag{8}$$

where $\mathbf{r}_j$ is the vector pointing to the center of sphere j.

Equations 7 and 8 can be reduced to discrete form by using the Kirkwood–Riesman theory, which was generalized by Dąbroś[33] to account for the presence of a wall. In discrete form, particle surfaces are divided into subunits and the integrations in eqs 7 and 8 is replaced by summation over these subunits. A more detailed discussion of the subunit method is presented elsewhere.[34]

The two particles in the collision are considered equal-sized spheres. One of them is free to move and rotate as a result of the external flow and forces acting on it, and the other one is held stationary on the wall. The force exerted on the subunits of each particle is chosen in such a way that the appropriate boundary conditions are satisfied at the particle surface. For the freely mobile particle the force, which consists of the interaction force between particles and possible external forces, has to be balanced by the hydrodynamic force. The same applies to torques acting on this particle. The inertia effects are expected to play no significant roles.

When the number of subunits for the two spheres is equal to N, eq 7 can be replaced by $6N$ linear equations plus six equations for the mobile particle expressing the balance of forces and torques. When the forces acting on the particle are specified, one can find $6N$ force components acting on the subunits and six components of the translational and rotational velocities. A sum of proper force components acting on the stationary particle provides information on the hydrodynamic force to which the

(31) Blake, J. R. *Proc. Cambridge Philos. Soc.* **1971**, *70*, 303.
(32) Dabros, T. *J. Fluid Mech.* **1985**, *156*, 1.
(33) Dabros, T. *Colloids Surf.* **1989**, *39*, 127.
(34) Dabros, T.; van de Ven, T. G. M. *J. Colloid Interface Sci.* **1992**, *149*, 493.

particle is subjected. In our calculations we match the numerical solutions with the analytical lubrication theory solutions[36-41] for small interparticle and/or particle−wall separations.

In the creeping flow limit the translational and rotational velocities of a particle (u_i and ω_i) are linear functions of the total forces and torques (f_i and t_i). Following Brenner's notation,[35] the generalized velocity $\mathbf{U} = \{u_1,u_2,u_3,\omega_1,\omega_2,\omega_3\}$ and force $\mathbf{F} = \{f_1,f_2,f_3,t_1,t_2,t_3\}$ acting on the freely mobile particles are related by

$$\mathbf{U} = \mathbf{M}\cdot\mathbf{F} \tag{9}$$

where $\mathbf{M}$ is the symmetrical, second-order mobility tensor of dimension 6 × 6. The resistance matrix $\mathbf{R}$ is defined as the inverse of the mobility matrix: $\mathbf{R} = \mathbf{M}^{-1}$. From eq 9 it follows that $\mathbf{F} = \mathbf{R}\cdot\mathbf{U}$.

The mobility and hence the resistance matrices depend on the viscosity of the fluid and geometry of the system. For two spherical particles near a wall, the components of $\mathbf{M}$ can be calculated from the response of a particle to a unit force and torque in a quiescent fluid. For small separations, expressions from lubrication theory can be used for the components of $\mathbf{M}$.[34]

With known expressions for the mobility tensor, for the hydrodynamic force acting on the moving particle at any given position, and for the interaction forces between two particles and between the moving particle and the wall, the trajectory equation (eq 1) can be solved numerically. Details of the calculations can be found elsewhere.[34]

Experimental Section

In this section we discuss some experiments with the surface collision apparatus. Because of its distinctive advantages over the traveling microtube apparatus, we no longer use the latter for the observation of particle collisions.

1. Materials. Two systems were studied. In one system we used 3.4 μm polystyrene latex particles, supplied by Dow Chemicals, in a glycerol (28% by weight)−water solution. In the other system we used 5 μm polystyrene−DVB latex particles, supplied by Duke Scientific, in a D_2O (60% by volume)−water mixture.

The ionic strengths of the two solutions were adjusted by the addition of KCl to 10^{-4} and 10^{-3} M, respectively. The glycerol was used to suppress the Brownian motion of the particles as well as to prevent them from sedimentation. D_2O was used only to prevent the sedimentation. The Brownian motion effect was reduced by using bigger particles (5 μm).

2. Setup and Procedures. The diagram of the surface collision apparatus is shown in Figure 7. The latex suspension is contained between two parallel plates placed at a distance of 150−200 μm from each other. The upper plate is transparent to enable observation with an optical microscope. It is attached to an *x*-*y*-*z* manual manipulator for accurate positioning. The lower plate is the bottom of a sample cell in which the suspension is contained. It is mounted on the platform of an electronic *x*-*y* manipulator which can be either driven by an IBM 386 computer or controlled manually with a joystick. The movement of the bottom plate creates a wall shear flow in the gap between the two plates. Since the ratio of the gap and the size of the plate is of the order of 0.001, at the center of the plate the edge effects which could disturb the flow pattern can be neglected.

The first step of the experiment is to find a stationary particle stuck to the upper plate due to random collisions between the particle and the plate. Then the bottom plate is moved with a joystick to bring any mobile particle in close vicinity of the stationary particle. After the mobile particle is positioned, we set the movement speed of the electronic manipulator to obtain the desired value of the shear rate and let these two particles collide (cf. Figure 8). The collision can be monitored and recorded with a video monitor, a VCR, and a video camera mounted to an optical microscope (Zeiss Axioplan). The same procedure is repeated to obtain a sufficient number of collisions required to invert the trajectory equation.

A typical picture of a collision is shown in Figure 9. Subsequent parts of the figure represent three stages of a particle trajectory: before, during, and after collision. For the purpose of the numerical analysis presented in the previous sections, we are only interested in the initial and final parts of the trajectory, i.e., when the distance between the two particles exceeds 6 radii. At such a separation distance the particle moves along a straight line in the direction of the flow since its motion is not influenced by the presence of the stationary particle. From the analysis of the motion of the moving particle, we can find two coordinates *x* and *z* perpendicular to the direction of shear (cf. Figure 1). This is done by analyzing the recording of the collision using an image processing technique. The video signal containing the process

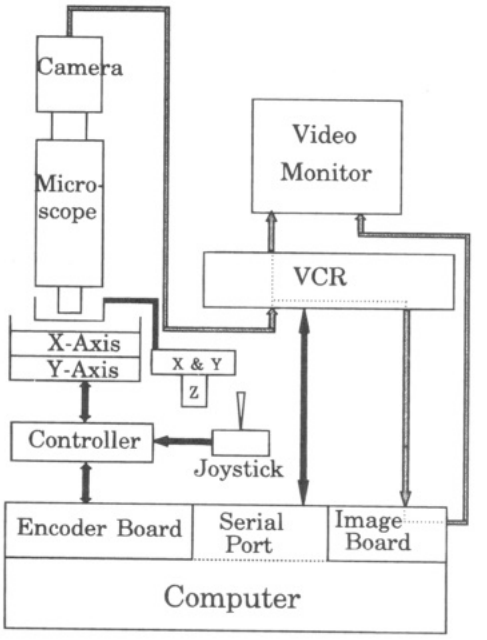

Figure 7. Setup of a surface collision apparatus. A wall shear flow is generated by moving the *x* and *y* axes of an electric micromanipulator (or encoder stage). The particle collisions occurring in the flow are observed under the microscope and recorded with the video camera and VCR. The collision trajectories are analyzed by the image processing board plugged into the computer.

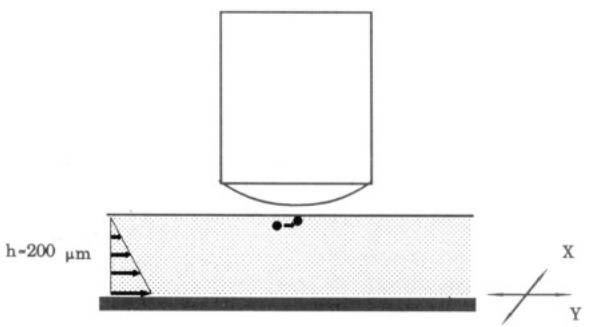

Figure 8. Particle collision in the sample cell. The upper plate remains stationary during a collision. The lower plate, which is mounted on the platform of the electric manipulator, moves at a velocity set by the computer. The gap width, *h*, is usually adjusted to be approximately 200 μm. A wall shear flow with certain shear rate is thus generated. The mobile particle moves in the shear flow and collides with the stationary particle stuck to the upper plate. Its initial positions can be accurately controlled by moving the *x*−*y* manipulator with a joystick.

(35) Brenner, H. *Adv. Chem. Eng.* **1966**, *6*, 287.
(36) Goldman, A. J.; Cox, R. G.; Brenner, H. *Chem. Eng. Sci.* **1967**, *22*, 637.
(37) Goldman, A. J.; Cox, R. G.; Brenner, H. *Chem. Eng. Sci.* **1967**, *22*, 653.
(38) Jeffrey, D. J.; Angew, Z. *Math. Phys.* **1984**, *35*, 634.
(39) O'Neill, M. E.; Stewardson, K. *J. Fluid Mech.* **1967**, *27*, 705.
(40) Jeffrey, D. J.; Onishi, Y. *J. Fluid Mech.* **1984**, *139*, 261.
(41) Cox, R. G.; Brenner, H. *Chem. Eng. Sci.* **1967**, *22*, 1753.

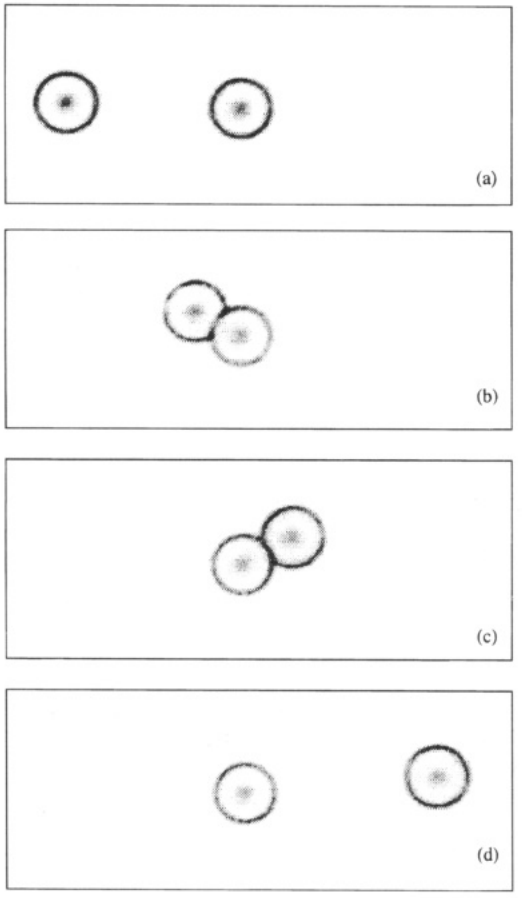

Figure 9. Snapshots of different stages of a particle collision. (a) The first stage: before collision. (b) The second stage: during collision. The moving particle is approaching the stationary particle. (c) The second stage: during collision. The moving particle is receding. (d) The third stage: after collision.

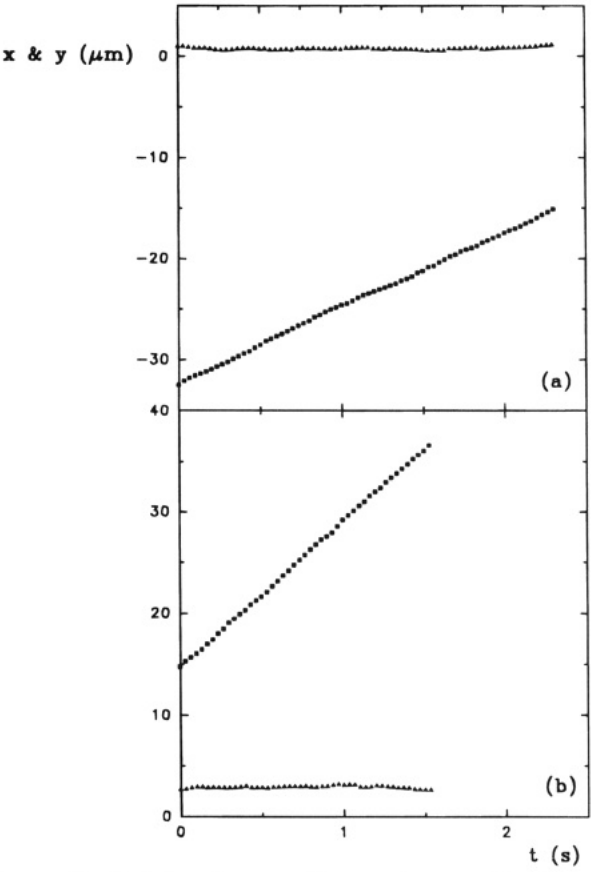

Figure 10. Position changes of the moving particle during a collision. The triangles stand for the x-coordinate, and the squares stand for the y-coordinate. The stationary particle is at position (0,0). (a) The position of the moving particle as a function of time before a collision. (b) The position of the moving particle as a function of time after a collision.

of a collision is digitized by a PC Vision Plus video analyzing board (Imaging Technology) plugged into the IBM 386 computer. From each video frame, the positions of the particles are extracted. Proper calibration of the image enables us to express the distance between particles in micrometers. Since the VCR (JVC BR-S605U) is computer-driven, frame analysis proceeds automatically from the moment the moving particle enters the monitor screen till the moment when the distance between the moving particle and the stationary particle is equal to 6 particle radii. This procedure yields the required information about the position of the moving particle prior to the collision (initial position). The video frame analysis is then interrupted during the moment of collision and resumed after the collision when the distance between particles exceeds, again, 6 particle radii. The analysis is continued until the moving particle leaves the monitor screen, yielding the information about the position after the collision (final position). A typical graph illustrating the changes of the moving particle positions before and after the collision is shown in Figure 10. Since the particle moves in the direction of shear, the x-coordinate perpendicular to shear remains unchanged, and the y-coordinate along shear changes linearly with time, yielding the particle velocity. The scattering of the particle positions around the straight lines is the result of Brownian motion and external noise (even though the whole setup is placed on a vibration-free table to minimize the influence of external noise).

It is evident from Figure 10 that the x-coordinate before and after the collision can be measured directly. In principle, the distance of a particle to a wall (z-coordinate) can be determined either by hydrodynamics[17] or by total internal reflection microscopy (TIRM)[18] or by reflection interference contrast microscopy (RICM).[19] The hydrodynamic method is the simplest one for obtaining the distance between a particle and a wall since it only needs measurements of the particle velocity and the shear rate. The former has already been given by the analysis of the y-coordinate varing with time. The shear rate can be simply calculated by dividing the manipulator speed by the gap width between the two parallel plates. Hence, we chose the hydrodynamic method to determine the z-coordinate in the CPS method. The procedure is as follows. The velocity of a sphere V_p moving in the vicinity of the wall in a shear flow is given by

$$V_p = f(H)\,\mathrm{G}z \tag{10}$$

where $H = (z - a)/a$ and $f(H)$ is a correction function accounting for the influence of the wall on the motion of the particle given by refs 37 and 42–44. We have tabulated $f(H)$, according to the expressions given by O'Neil and co-workers[42–44] at 60 distances (note that a factor of 0.5 is missing in eq 4.24 in ref 44). At other distances $f(H)$ can be calculated by cubic spline interpolation. After the velocity of the moving particle has been found, we can invert eq 10 to find the distances between the particle and the wall (z-coordinate) before and after the collision. The z-coordinate determined in this way is very accurate. The error is usually around 3% of the particle radius. The x-coordinate is even more accurate because it can be directly measured.

After the initial and final positions of the moving particle for all collisions recorded in the experiment have been found, we can plot them in a "scattering pattern" (see Figure 2 and also Figure 11 for details). The scattering pattern is a convenient way of presenting experimental data. It also provides some information about the properties of a system even before the parameter fitting is performed.

Finally, we proceed with the trajectory inversion calculation presented above to obtain the interaction force–distance profile.

Results and Discussion

Figure 11 shows the scattering pattern obtained for 25 collisions in the glycerol–water system. The open circles

(42) Dean, W. R.; O'Neill, M. E. *Mathematika* **1963**, *10*, 13.
(43) O'Neill, M. E. *Mathematika* **1964**, *11*, 67.
(44) Goren, S. L.; O'Neill, M. E. *Chem. Eng. Sci.* **1971**, *26*, 325.

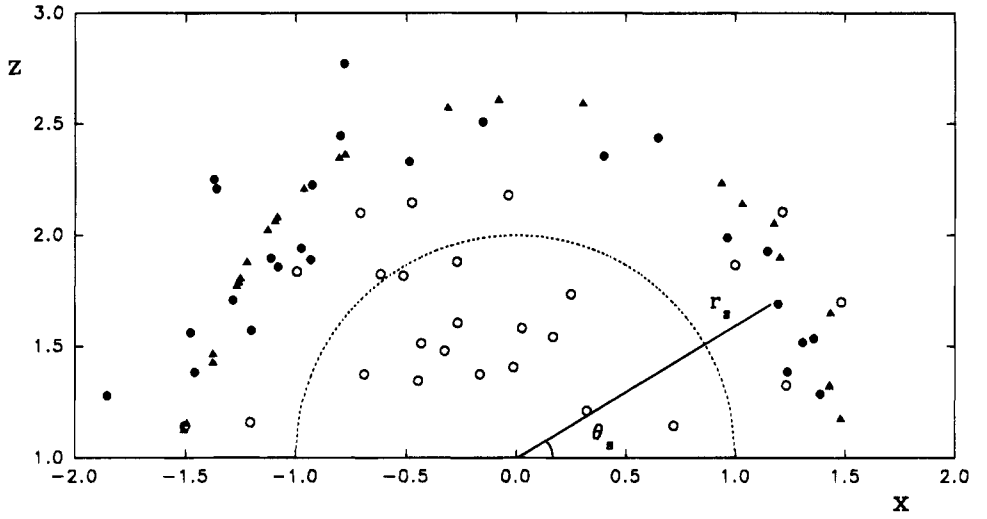

Figure 11. Scattering pattern of 3.4 μm latex particle collisions in a 28% glycerol–water solution with 10^{-4} M KCl. The coordinates are scaled by the particle radius. The open circles represent the initial positions of the moving particles. The filled circles represent the experimentally determined final positions of the particles. The filled triangles stand for the theoretically calculated final positions of the particles. The semicircle in the middle is the projection shadow of the stationary particle.

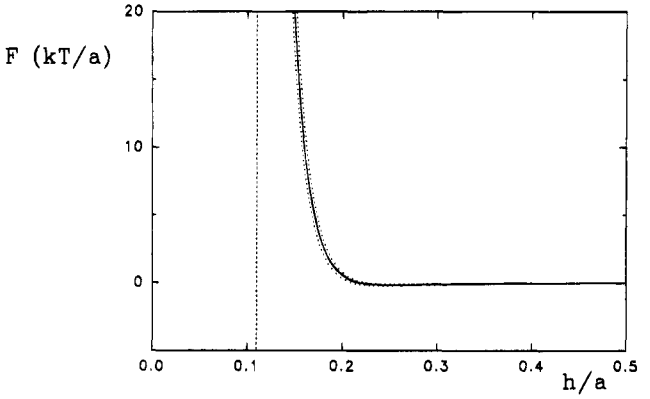

Figure 12. Fitted interaction force vs interparticle distance profile in a 28% glycerol–water solution with 10^{-4} M KCl. The distance has been scaled by the particle radius (a = 1.7 μm). The force has been scaled by kT/a. The solid line is the force–distance curve. The dotted lines are the confidence intervals at the 90% confidence level. The dashed line on the left is the minimum separation distance between the two particles observed in the experiment. The fitted Hamaker constant, A, is 2.1×10^{-20} J, and the fitted surface potential, ψ_0, is −54 mV.

stand for the initial positions of the moving particle, and the filled circles are the final positions of the particle. The semicircle in the middle is the projection "shadow" of the stationary particle. It can be seen that all trajectories that start within the semicircle or close to it end up much further away from it. This indicates that there is a strong repulsive force acting between two particles, which was confirmed when we applied the minimization procedure to obtain the interaction force as a function of interparticle distance. As a test function, we assumed that the force–distance relationship was given by DLVO theory (cf. eq 4) with three adjustabe parameters: the dimensionless double layer τ, the double-layer interaction parameter Dl, and the scaled Hamaker constant Ad. The retardation parameter Al was kept constant at a value corresponding to λ = 100 nm. The resulting force profile is shown in Figure 12. The best fit gives double-layer thickness $1/\kappa$ = 28.5 nm, Hamaker constant $A = 2.1 \times 10^{-20}$ J, and surface potential $\psi_0 = -54$ mV. The surface potential is in good agreement with the ζ-potential, $\zeta = -51$ mV measured with a microelectrophoresis apparatus (Rank Brothers, Cambridge, England). The double-layer thickness also agrees with the theoretical value, 28.9 nm, calculated from the ionic strength of the solution. The fitted force profile describes a strong electrostatic repulsion with a shallow secondary minimum. The dotted lines indicate the 90% confidence intervals for the force profile. The accuracy of the procedure will be discussed in more detail below.

After the interaction force profile has been obtained, one can solve again the trajectory equation for the experimentally given initial positions to calculate the "theoretical" final positions and then compare them with the experimental final positions. The filled triangles in Figure 11 are these theoretical positions. The differences between them and experimental final positions can be attributed to the influence of Brownian motion, the instrumental error in measuring particle positions, misalignment, and slight vibration of the system. Polydispersity of the sample can also contribute to the error since all calculations are performed in dimensionless units scaled by the particle radius, assumed identical for both particles. Among all of these errors, Brownina motion is the most serious one. Other errors are either small or can be eliminated under certain conditions. As mentioned earlier, there are two kinds of Brownian motion effects. The effect to the particle position measurement can be minimized by a selection criterion which discards collisions with a difference in the directions of approaching and receding trajectories greater than 1°. The effect to the collision trajectory can be minimized by selecting collisions with a scattering angle, θ_s, (see Figure 11 for definition) similar to the one predicted by the hydrodynamic theory. This selection criterion does not affect the choice of force parameters because it has been found by experience that the force profile mainly changes the radial scattering distance, r_s. The scattering angle almost solely depends on the hydrodynamics. In the case of the experiments with the glycerol–water system, the 25 collisions used for fitting were selected from 80 observed collisions using these criteria.

The same experiment was carried out in a D_2O–water system. The scattering pattern is shown in Figure 13. The meaning of symbols is the same as in Figure 11. Before we started the Marquart–Levenberg fitting, we studied the topology of χ^2 of this system using bicubic spline interpolation from 54 grid points. The resulting contour map of χ^2 (cf. Figure 14) shows two minima (near χ^2 = 17.6 and 17.8) and one flat valley around $\psi_0 = -40$ mV and $A = 2 \times 10^{-20}$ J. The minimum surrounded by the 17.6

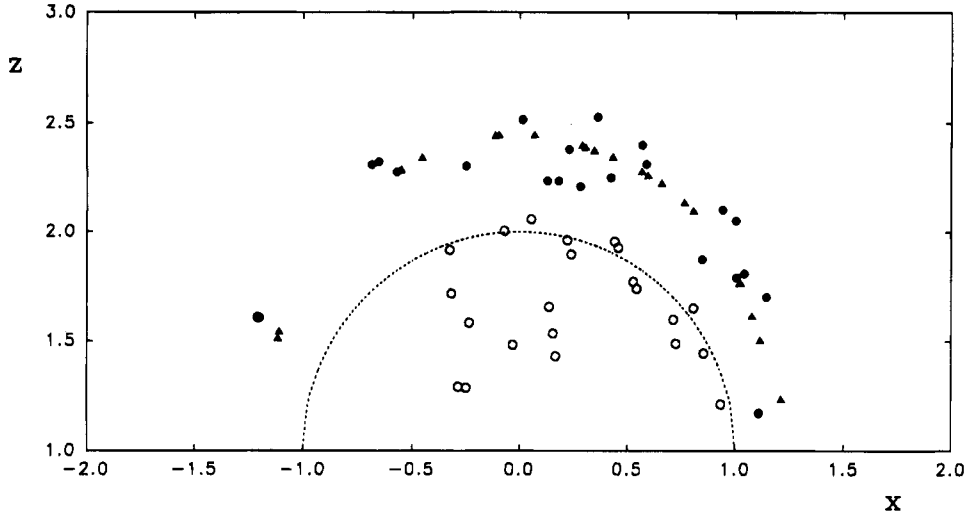

Figure 13. Scattering pattern of 5 μm latex particle collisions in a 60% D_2O–water mixture with 10^{-3} M KCl. The coordinates are scaled by the particle radius. The meaning of the symbols is the same as in Figure 10.

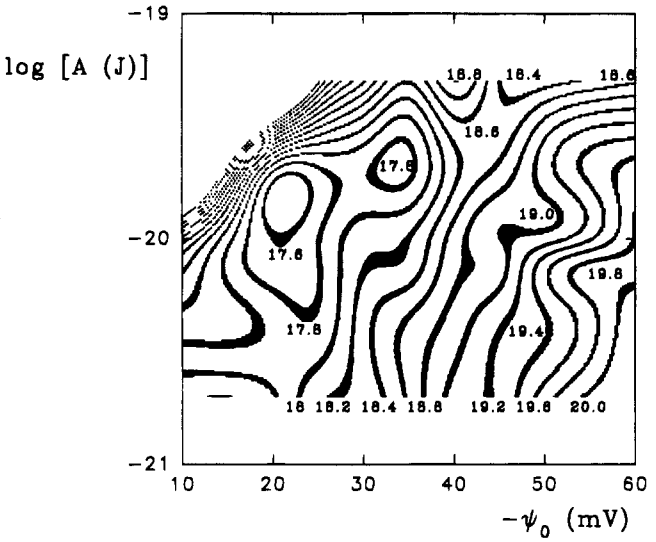

Figure 14. χ^2 contour map of the fitting of 5 μm latex particle collisions in a 60% D_2O–water mixture with 10^{-3} M KCl. The numbers on the graph are χ^2 values. The double-layer thickness $1/\kappa$ is fixed according to the calculated value, 30 nm. ψ_0 is the surface potential, and A is the Hamaker constant.

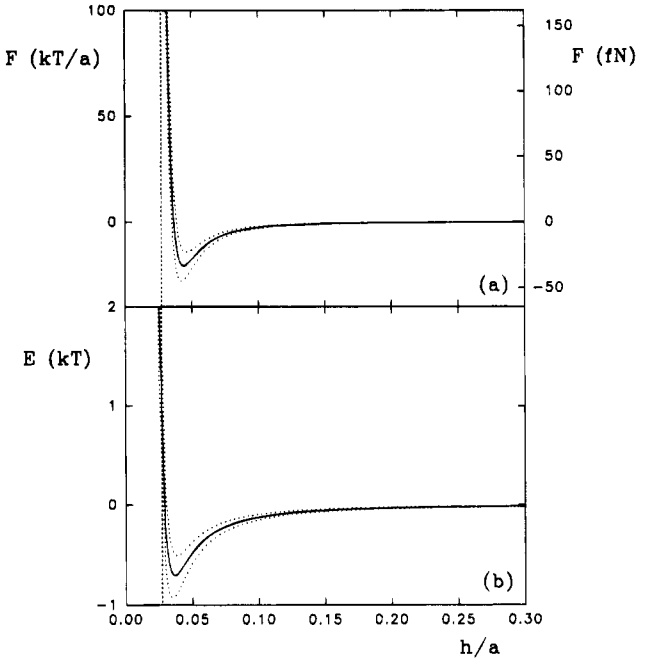

Figure 15. (a) Fitted interaction force vs interparticle distance profile in a 60% D_2O–water mixture with 10^{-3} M KCl. The distance has been scaled by the particle radius (a = 2.5 μm). The force is presented both in dimensionless form scaled by kT/a and in dimensional units, fN (10^{-15} N). The solid line is the force–distance curve. The dotted lines are the confidence intervals at the 90% confidence level. The dashed line on the left is the minimum separation distance (about 75 nm) between the two particles observed in the experiment. The fitted Hamaker constant, A, is 2.0×10^{-20} J, and the fitted surface potential, ψ_0, is −33 mV. (b) Fitted interaction energy vs interparticle distance profile integrated from the above force profile. The energy has been scaled by kT. The meanings of different curves and lines are the same as above.

contour circle ($\psi_0 = -22$ mV and $A = 1.4 \times 10^{-20}$ J) is too far away from the experimental ζ-potential, $\zeta = -42$ mV. The flat valley was not chosen because the value of χ^2 (18.4) is relatively large. Hence, the minimum surrounded by the 17.8 contour circle ($\psi_0 = -32$ mV and $A = 2 \times 10^{-20}$ J) is the only one which provides a good fit to the data. The starting point of the Marquart–Levenberg fitting was thus chosen within the circle to prevent trapping in other inappropriate local minima.

The values of the best fit parameters are the Hamaker constant $A = 2.0 \times 10^{-20}$ J and the surface potential $\psi_0 = -33$ mV. The corresponding force profile is shown in Figure 15a. Both of the two parameters agree reasonably well with the theoretical Hamaker constant $A = 9.5 \times 10^{-21}$ J calculated from spectroscopic data[45] and the ζ-potential $\zeta = -42$ mV measured by microelectrophoresis.

It is of interest to compare the experimental Hamaker constant with the theoretical Hamaker constant $A = 9.5 \times 10^{-21}$ J, since one hypothesis[46] suggests that there is a long-range hydrophobic interaction force between hydrophobic bodies (like two latex spheres). If hydrophobic forces were operating, the apparent Hamaker constant should be at least an order of magnitude larger than the theoretical one. The experimental Hamaker constant determined here with CPS together with the results of Figures 6 and 12 does not show the existence of such a hydrophobic force between two latex spheres, at least not for distances larger than about 75 nm. The slightly bigger

(45) Hunter, R. J. *Foundations of Colloid Science*; Clarendon Press: Oxford, 1989; Vol. 1.

(46) Ninham, B. W. Plenary Lecture at 67th Colloid and Surface Science Symposium, Toronto, 1993.

value of the measured Hamaker constant can be explained by the experimental error and the influence of the surface roughness of the particles which increases the apparent van der Waals attraction.[47]

It is worth noting that, when we express the interaction force profile in dimensional units (cf. Figure 15a), the magnitude of the force measured with our method is on the order of 10^{-14} N, which is 3–4 orders of magnitude smaller than the minimum force that can be detected by SFA or AFM. If we transform this force into a corresponding interaction energy, we obtain an energy of the order of kT (cf. Figure 15b), which is a typical depth of the secondary energy minimum in a stable colloidal system. With this sensitive force detection ability, some useful properties of a colloidal system can thus be predicted from the force measurement.

Conclusion

In this paper we presented a new method to determine interaction forces between colloidal particles. The advantage of this method over other force measurement methods is that it determines the forces acting between two colloidal particles during a collision—a dynamic process taking place repeatedly in a real colloidal system and playing a key role in its stability as well as its rheological behavior. The forces determined in such a way can thus be used to predict the properties of a colloidal system. The method is based on the inversion of the trajectory equation that governs the relative motion of particles in a shear flow. From the experimentally determined positions of two particles before and after a collision, we can find the parameters describing the dependence of the interaction force upon distance between these two particles. This is achieved by minimizing the differences between the experimentally determined final positions of particles and the final positions calculated from respective experimental initial positions by solving the trajectory equation.

The Monte Carlo simulations show that approximately 25 collisions are required to obtain a reliable force–distance curve. The traveling microtube technique, which was used previously to study collisions of colloidal particles, fails to offer such a number of collisions in a single experiment. Nevertheless, some meaningful results can be obtained by applying our minimization technique to the existing traveling microtube data.

A new experimental technique, the surface collision apparatus, has been developed to replace the traveling microtube technique. It is based on the observation of collisions between two particles in a wall shear flow. Although the theoretical analysis of the hydrodynamic problem in this case is much more complicated than that in a simple shear flow (the system of the traveling microtube), the experimental technique has proven to be far more efficient than that of the traveling microtube. With the aid of a fast computer, the problem of the theoretical analysis can also be solved.

Preliminary results of the interaction forces between polystyrene latex particles in mixtures of glycerol–water and D_2O–water prove the usefulness of the technique. Furthermore, they indicate that the method is much more sensitive than SFA and AFM methods. It is capable of determining a force corresponding to an interaction energy of less than a single kT.

(47) Czarnecki, J. *Adv. Colloid Interface Sci.* **1986**, *24*, 283.